Research Article

Received: 16 December 2014 Revised: 23 March 2015 Accepted article published: 26 May 2015 Published online in Wiley Online Library: 15 June 2015

(wileyonlinelibrary.com) DOI 10.1002/pi.4939

Effect of hydrothermally synthesized titanium nanotubes on the behaviour of polypropylene for antimicrobial applications

Andrés Zenteno,[a] Sichem Guerrero,[b] María Teresa Ulloa,[c] Humberto Palza[d] and Paula A Zapata[a]*

Abstract

TiO_2 nanotubes (TiO_2-Ntbs) synthesized by a hydrothermal method were used as filler to prepare polypropylene (PP) composites by melt blending. Their structural properties as well as their biocidal potential were studied. Nanotubes were used either as-synthesized or organically modified with hexadecyltrimethoxysilane (Mod-TiO_2). These nanoparticles form secondary structures with sizes around 100 nm that are well dispersed in the polymer matrix, but not homogeneously because agglomerates larger than 1 μm are also seen by transmission electron microscopy. Regarding the properties of the composites, the incorporation of the nanoparticles increased the polymer's crystallinity and thermal stability. The maximum decomposition temperature of the matrix increased by *ca* 13 °C compared to virgin PP. The nanotubes further increase the spherulite nucleation density, and therefore a reduction in the diameter of spherulites and an increase in their number were observed. Despite the above, the addition of TiO_2 nanoparticles did not modify the mechanical properties of PP. The PP/TiO_2-Ntb nanocomposites exposed to UVA radiation showed a biocidal behaviour, reducing a colony of *Escherichia coli* by 81%.

Keywords: polymer – matrix composites (PMCs); particle reinforcement; optical properties/techniques; thermal analysis; moulding compounds

INTRODUCTION

Polyolefins, such as polyethylene (PE) and polypropylene (PP), are of particular interest as they allow the production of inexpensive and commodity materials for use in a wide range of applications.[1] The addition of small amounts (1 – 10 wt%) of nanoparticles can modify the behaviour of polyolefins, allowing further development of novel materials. Compared with polymer/microparticle composites, nanocomposite materials have improved properties at much lower filler concentrations, including crystallization, mechanical strength, melt processing, electrical and thermal conductivity, thermal degradation stability and viscoelasticity, among others.[2,3] Different types of nanoparticles such as modified clay,[4] SiO_2,[5] carbon nanotubes, graphite[6] and TiO_2[7,8] have been introduced into polymers to study their influence on the final properties of the nanocomposite produced. Among them, TiO_2 is one of the most important materials due to a variety of possible applications and attractive multi-functional behaviours that can be obtained.[9] TiO_2 has a great potential in different areas such as photoelectric conversion in solar cells,[10] environmental purification, decomposition of carbonic acid gas and generation of hydrogen gas.[11] In particular, TiO_2 has photocatalytic properties, generating reactive species under UV irradiation, such as hydroxide superoxide radicals capable of degrading cell components of microorganisms, and therefore acting as anti-bacterial agents.

In order to improve the thermal and mechanical properties, and to add biocidal characteristics, TiO_2 nanoparticles with quasi-spherical or spherical morphology have been incorporated into different polyolefin matrices such as high density PE,[12] low density PE, polystyrene[13] and PP.[14]

These polyolefin-based antimicrobial materials are of great industrial interest where infections are relevant due to their extensive use in textiles, food packaging and others. This is why currently important research is being done on the possibility of adding bactericidal properties to these materials.

Joseph and colleagues[15] obtained PP/TiO_2 composites by the melt mixing method using particles around 20 nm in size. The mechanical properties of PP fibres were enhanced by adding TiO_2 nanoparticles (3 wt%), and calorimetric studies showed an increased degree of crystallization, indicating

* *Correspondence to: P. A. Zapata, Grupo Polímeros, Facultad de Química y Biología, Universidad de Santiago de Chile, USACH, Casilla 40, Correo 33, Santiago, Chile. E-mail: paula.zapata@usach.cl*

a *Grupo Polímeros, Facultad de Química y Biología, Universidad de Santiago de Chile, USACH, Casilla 40, Correo 33, Santiago, Chile*

b *Facultad de Ingeniería y Ciencias Aplicadas, Universidad de los Andes, Monseñor Álvaro del Portillo 12455, Las Condes, Santiago, Chile*

c *Programa de Microbiología y Micología, ICBM-Facultad de Medicina Universidad de Chile, dirección, Avenida Independencia 1027, Comuna Independencia, Santiago, Chile*

d *Departamento de Ingeniería Química y Biotecnología, Facultad de Ciencias Físicas y Matemáticas, Universidad de Chile, Beauchef 850, Santiago, Chile*

that TiO_2 nanoparticles are acting as nucleating agents for PP crystallization.

Cerrada and colleagues[16] also incorporated anatase-TiO_2 nanoparticles into isotactic PP by the melt mixing process with concentrations between 0.5 wt% and 5 wt%. The characterization of the PP/TiO_2 nanocomposites provides evidence of good dispersion of the filler in the polymer matrix despite the absence of significant changes in the structural properties of the polymer. The nanocomposites with loads less than 2 wt% of TiO_2 showed antimicrobial activity.

The ability to inactivate *Escherichia coli* in lettuce packaging using oriented PP film (OPP) coated with TiO_2 nanoparticles has also been studied.[17] The TiO_2-coated OPP film without light illumination did not show any activity against *E. coli*. The extent of *E. coli* inactivation by TiO_2-coated OPP film is related to UVA intensity and the type of artificial light source. The photocatalytic disinfecting activity of TiO_2-coated OPP film under black light bulb illumination (UVA) was higher than under fluorescent light. The same authors investigated and found antifungal activity of TiO_2 using a photocatalytic reaction and TiO_2 powder and TiO_2 coated on PP film against *Penicillium expansum,* which is one of the most important post-harvest fungal problems in fruits and vegetables.[18]

One disadvantage of the synthesis of the nanocomposites with polyolefins is the tendency of the particles to agglomerate, which in turn results in polymers with poor properties. This can be improved by a surface modification of the TiO_2 particles. Altan and Yildirim[19] used two methods to obtain these modifications: one was by coating the TiO_2 with an elastomer phase based on maleic anhydride grafted styrene-ethylene-butylene-styrene (SEBS-*g*-MA) and silane compounds; the other method was by coating the nanoparticles only with silane groups. After modification, the nanoparticles were incorporated by melt compounding into the PP matrix. The SEBS-g-MA and silane-coated TiO_2 nanoparticles provided higher mechanical and biocidal properties than TiO_2 nanoparticles modified with silane only, showing the surface adhesion enhancement between matrix and particles. Zohrevand *et al.*[20] prepared nanocomposites based on isotactic PP (iPP) and TiO_2 nanoparticles (4.6–45.5 wt%) prepared by the melt blending process. In order to improve interaction between the polymer and the particles, anhydride-modified PP was used as a compatibilizer. It was shown that the thermal stability and crystalline structure of the nanocomposite are significantly affected by the particles' state of dispersion. TiO_2 nanoparticles were shown to be strong β-nucleating agents for iPP, especially at low concentrations. Recently, titanate nanotubes (TiNTs) were mixed with modified PP by a batch melt mixing procedure. PP modified by irradiation with high-energy electrons was used to increase the compatibility between polymer and nanoparticles. The microstructure of the PP/TiNT nanocomposites shows well-dispersed TiNTs and some aggregates (clouds) in the polymer. The enhancement of the mechanical properties shows that TiNTs can be used as an efficient filler in non-polar polymers using polymers modified by irradiation. The biocidal properties were not studied.[21]

As already mentioned, studies of the mechanical, thermal and biocidal properties of polymer/TiO_2 nanocomposites have been carried out using spherical fillers. However, the use of TiO_2 nanotubes (TiO_2-Ntbs) has been little reported so far in the related literature, even though the strong effect of the filler aspect ratio on the behaviour of the matrix, such as the crystallization processes or the morphology as reported for SiO_2 nanoparticles in a PP matrix, is well known. Therefore, the high aspect ratio of nanotubes compared to nanospheres may have a positive effect on the final properties of the PP.[22]

Considering the above, in the present work we study the organic modification of TiO_2-Ntbs to improve their interaction with the non-polar matrix. The effect of different amounts of TiO_2-Ntbs and modified TiO_2-Ntbs (Mod-TiO_2-Ntbs) on the thermal, mechanical and crystallization properties of PP was studied. The antimicrobial behaviour of these PP/TiO_2-Ntb nanocomposites against *E. coli* was also investigated.

EXPERIMENTAL

Materials

PP was purchased from Petroquim (Chile). The reagents used in the synthesis of the TiO_2-Ntbs were TiO_2 powder (anatase) provided by Aldrich, USA, nitric acid (HNO_3), sodium hydroxide (NaOH) pellets (Mallinckrodt Chemicals) (German) and distilled water. Hexadecyltrimethoxysilane (Aldrich, USA) was used for the modification of TiO_2-Ntbs (Mod-TiO_2-Ntbs).

Synthesis of titanium nanotubes (TiO_2-Ntbs) and their organic modification (Mod-TiO_2-Ntbs)

The hydrothermal treatment for the synthesis of TiO_2-Ntbs was based on reported methods.[23,24] Raw TiO_2 anatase powder (2.5 g) was mixed with 125 mL of 10 mol L^{-1} NaOH. This solution was placed in a sealed Teflon reactor and heated at 110 °C for 24 h, stirring every hour. The slurry was washed several times with distilled water (1 L) and then filtered. Then 150 mL of 0.1 mol L^{-1} HNO_3 solution was added to the powder and mixed during 24 h. This slurry was washed with 1 L of distilled water and the resultant powder was filtered, dried and calcined at *ca* 200 °C for 4 h.

The nanotubes were organic-modified with hexadecyltrimethoxysilane (Mod-TiO_2-Ntbs) as described previously.[12] TiO_2-Ntbs (2.0 g) were dissolved in ethanol and distilled water (ratio 2:1 vol/vol) and the solution was stirred for 2 h. A given amount of modifier was then added dropwise to the initial solutions and again stirred for 2 h at 25 °C. The mixture was washed with ethanol and finally heated to 120 °C in vacuum for 6 h to promote the chemical coupling.[25]

PP/TiO_2-Ntb and PP/Mod-TiO_2-Ntb nanocomposite preparation

The composites were prepared using a Brabender Plasti-Corder internal mixer at 190 °C and a speed of 110 rpm during 10 min. Predetermined amounts of the titanium nanoparticles and neat polymer (as received) were mixed in a nitrogen atmosphere in order to obtain nanocomposites with 5% wt/wt and 8% wt/wt of TiO_2-Ntbs nanofiller. The samples were press-moulded at 190 °C at a pressure of 50 bar for 3 min and cooled under pressure by flushing the press with cold water.

TiO_2-Ntbs and composite characterization

Characterization of the titanium nanotubes (TiO_2-Ntbs) and their organic modification (Mod-TiO_2-Ntbs)

Fourier transform infrared (FTIR) analyses of the TiO_2-Ntbs and Mod-TiO_2-Ntbs were performed in a Bruker Vector 22 FTIR spectrometer. The IR spectra were collected in the 4000 to 500 cm^{-1} range, with a resolution of 4 cm^{-1} at room temperature.

The X-ray diffraction patterns of the Mod-TiO_2-Ntbs were analysed on a Siemens D5000 diffractometer using Ni-filtered Cu Kα radiation ($\lambda = 0.154$ nm).

UV absorption spectra of the TiO_2-Ntbs and Mod-TiO_2-Ntbs in the 200 – 700 nm range were obtained on a UV Perkin Elmer Lambda 650 UV – visible spectrometer.

PP/TiO_2-Ntbs and PP/Mod-TiO_2-Ntbs characterizations

The melting temperature and enthalpy of fusion of the neat and nanocomposite PP samples were measured by DSC (TA Instruments DSC 2920). The samples were heated from 25 °C to 180 °C at a rate of 10 °C min^{-1} and then cooled to 25 °C at the same rate. The values were taken from the second heating curve to eliminate any thermal history. The percentage crystallinity was calculated using the enthalpy of fusion of an ideal PP with 100% crystallinity (207 J g^{-1}).[26] For the nanocomposites it was calculated as described previously, but taking into account the weight of the nanotubes.[27]

The polymer's thermal stability was evaluated by TGA using a Netzsch TG Libra 209 instrument in an inert atmosphere (nitrogen). The samples were heated from 25 °C to 600 °C at a rate of 20 °C min^{-1}.

Polymer viscosity was measured by dissolving the polymer in decalin at 135 °C in a Viscosimatic-Sofica viscometer.

The isothermal spherulite growth rate of neat PP and its nanocomposite was studied under a Leica DML optical microscope with polarized light coupled with a Linkam Scientific Instruments TMS94 heating stage controlled by a Linkam LTS 350 system. Thin sample pieces placed under a cover glass on a microscope slide were heated to 190 °C and kept for 2 min. The samples were then cooled from 190 °C to a given crystallization temperature.

The morphology of the TiO_2-Ntbs and their dispersion in the composites were analysed by TEM (JEOL ARM 200 F) at 20 kV.

The tensile properties of the polymer and composites were determined on a model D-500 Hewlett Packard dynamometer. The materials were moulded for 4 min in a hydraulic press (Hewlett Packard Industrial Instruments) at a pressure of 50 bar and a temperature of 190 °C, and then cooled under pressure by flushing with water. Films around 0.05 mm thickness were obtained. Dumbbell-shaped samples with an effective length of 30 mm and 5 mm width were cut from the compression-moulded sheets. The samples were tested at a rate of 50 mm min^{-1} at 20 °C. Each set of measurements was repeated at least four times.

The antimicrobial effect of the different samples was determined using the ISO 20143 plate count method. *E. coli* ATCC 25922 was used for the analysis. In brief, the initial number of bacteria present after incubation was calculated by counting the number of colonies in a 10× dilution. From a fresh culture, a microbial suspension of 1×10^5 colony forming units (CFU) mL^{-1} counted by a bioMérieux® Densimat was prepared in brain – heart infusion (BHI) broth plus Triton 100, in a humid chamber. The suspension (0.5 mL) was placed in contact with each 2.5-cm^2 sample (pure PP as control and PP/TiO_2-NTbs) for 4 h and further exposed to white light and UVA light (a couple of 8 W black light bulbs, Hitachi model FL-8BL-B). The UVA (315 – 400 nm) light intensity was 0.2 mW cm^{-2} as measured by a digital light meter (SLM-110, A.W. Sperry). Each sample (control samples and antibacterial-treated samples) was recovered by suspending in 10 mL of sterile saline and serially diluted 1/10, 1/100 and 1/1000. Then, 0.2 mL of each dilution was plated in duplicate on trypticase soy agar plates and incubated at 37 °C for 24 h. All biocidal properties were measured in triplicate, and after incubation the number of colonies in the Petri dishes was counted twice. The percentage of inhibition of microorganisms in the samples was determined according to their respective controls.

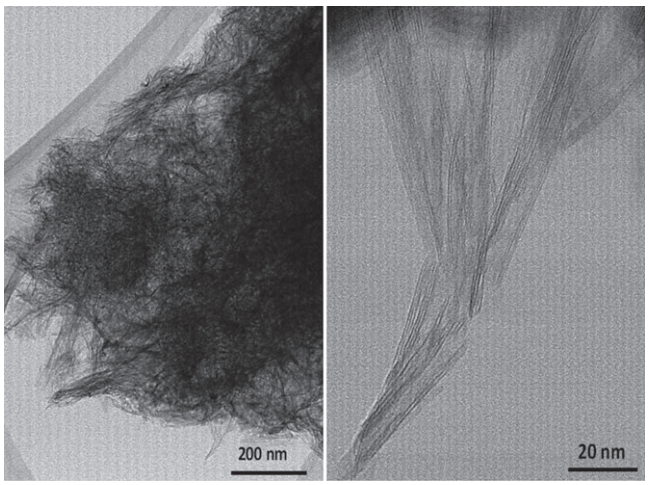

Figure 1. TEM images of titanium nanotubes (TiO_2-Ntbs).

RESULTS AND DISCUSSION

Characterization of titanium oxide nanoparticles (TiO_2-Ntbs and Mod-TiO_2-Ntbs)

Electron micrographs (Fig. 1) of TiO_2-Ntbs reveal a nanotube morphology with an average diameter of *ca* 5 nm. TiO_2 nanospheres of the raw material were not seen. These images confirm the high efficiency of this synthesis based on the method reported by Kasuga *et al.*[23] The crystalline phase of the TiO_2-Ntbs was analysed by XRD (Fig. 2(a)), showing Bragg reflections at about 25° and 48°, corresponding to the (101) and (200) planes, respectively, due to tetragonal crystals of TiO_2 anatase phase.[28,29] In addition, the XRD pattern of the TiO_2-Ntbs shows another peak at 11°, which corresponds to the characteristic diffraction of the (200) plane of TiO_2 titanate nanotubes.[30] The diffraction pattern of the TiO_2-Ntbs shows other peaks of lower intensity than those of anatase polymorphism, which have previously been attributed to the nanotube structures.[31]

TiO_2-Ntbs and Mod-TiO_2-Ntbs show UV absorption around $\lambda_g = 366$ nm and $\lambda_g = 375$ nm, respectively, attributed to valence electron band transitions characteristic of TiO_2, as shown in Fig. 2(b). According to the $E_g = 1239.6/\lambda_g$ equation,[32,33] the calculated band gap (E_g) energies were *ca* 3.38 eV for TiO_2-Ntbs and 3.31 eV for Mod-TiO_2-Ntbs. The E_g values of our TiO_2 nanotubes were slightly higher than the value reported for the anatase phase ($E_g = 3.1$ eV) with spherical morphology.[12] It is probable that the change in the morphology from nanospheres to nanotubes resulted in an increase of the band gap in the anatase crystalline structure.

Two types of TiO_2-Ntbs were synthesized to be used as filler: as-synthesized and surface modified with hexadecyltrimethoxysilane, with the latter having a greater hydrophobic character. The surface modification described in the Experimental section was achieved as reported previously.[7,12] The surface groups of TiO_2-Ntbs before and after modification were characterized by IR as shown in Fig. 3. The surface-modified TiO_2-Ntbs display new IR absorption peaks. These new signals are those typical of symmetric stretching at 2845 cm^{-1} and asymmetric stretching at 2950 cm^{-1}, both corresponding to CH_2 groups from the organic precursor. A shoulder appears at 930 cm^{-1}, which is related to the Si – O – Si anti-symmetric stretching of the silane compound.[34] Moreover, the Mod-TiO_2-Ntbs show a lower intensity in the 3000 – 3600 cm^{-1} range, which is characteristic of surface hydroxyls. The

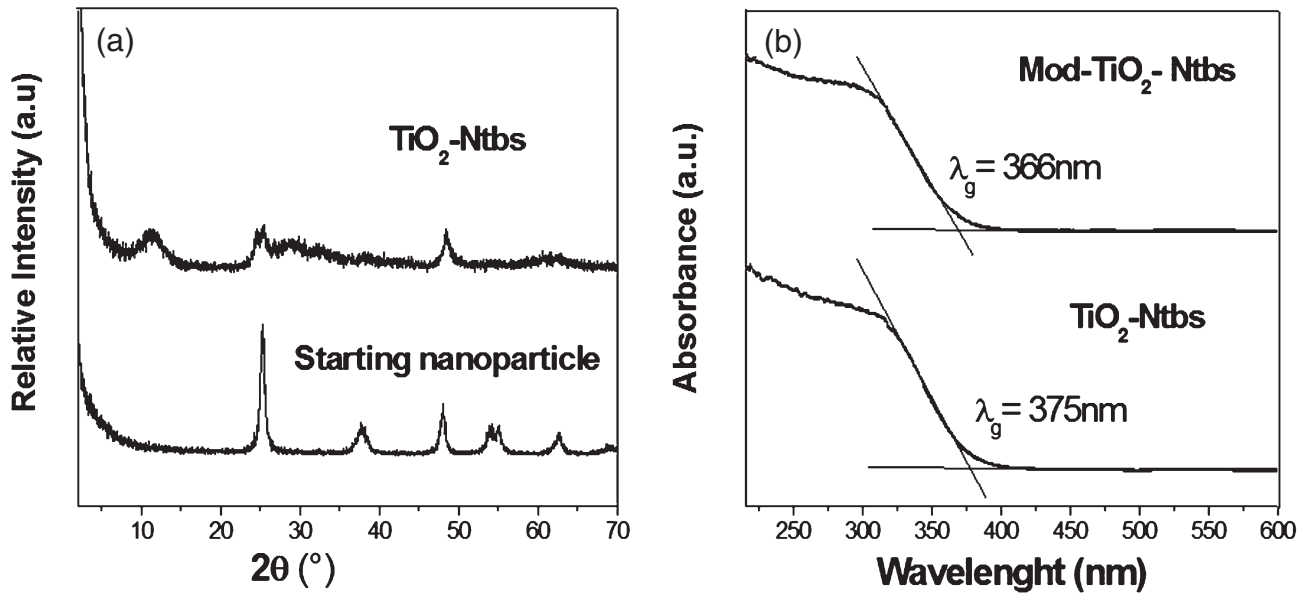

Figure 2. (a) XRD of TiO_2-Ntbs and the starting nanoparticles from Aldrich. (b) UV – visible spectra of TiO_2-Ntbs and Mod-TiO_2-Ntbs.

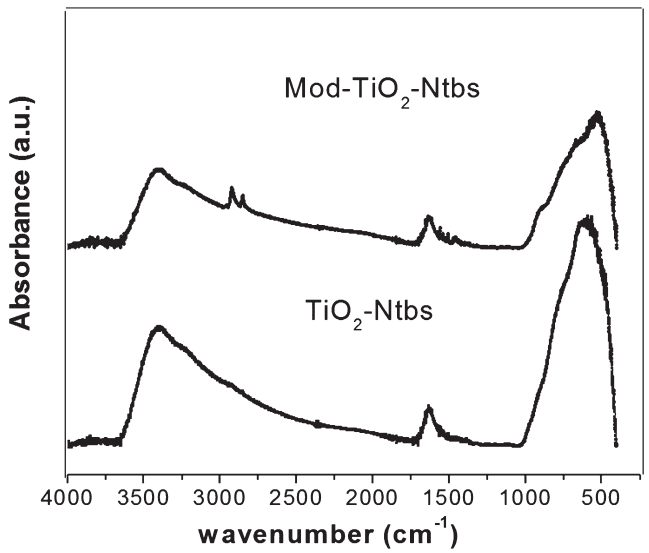

Figure 3. IR spectrum of TiO_2-Ntbs and Mod-TiO_2-Ntbs.

reaction between TiO_2 nanoparticles with silane molecules proceeds through different steps as reported previously.[12,35] Initially, the silane is hydrolysed in the presence of water, and then physical adsorption through hydrogen bonds occurs between OH groups of silanols and the TiO_2 surface. Finally, the grafting is carried out under heating conditions, with the hydrogen bonds between the silanols and the hydroxyl groups from TiO_2 being converted into covalent Si – O – C bonds, releasing water. These results confirm the occurrence of a chemical reaction between Ti–OH from the nanotubes and C–OH from the organic modifier.[36]

Characterization of the nanocomposites

Viscosity and thermal stability of the nanocomposites

The effect of incorporating 5 wt% and 8 wt% of nanotubes into PP on the viscosity and thermal properties of the nanocomposites is displayed in Table 1. The viscosity did not present any

Table 1. Viscosity and thermal properties of PP/TiO_2-Ntb and PP/Mod-TiO_2-Ntb nanocomposites

Composite	TiO_2 (wt%)	η (dL g^{-1})	T_m (°C)	X_c (%)	T_{10} (°C)	T_{max} (°C)
Pure PP	0	1.42	165	56	429	467
PP/TiO_2-Ntbs	5	1.47	164	61	455	476
	8	1.55	164	66	462	477
PP/Mod-TiO_2-Ntbs	5	1.54	164	64	463	480
	8	1.42	164	68	466	479

η is the intrinsic viscosity; T_m is the melting temperature; X_c is the percentage crystallinity; T_{10} is the decomposition temperature at 10% weight loss; T_{max} is the temperature for the maximum rate of weight loss (T_{peak}); Mod-TiO_2 are modified nanoparticles.

significant change, showing that the molecular weight was unchanged during composite formation or with the presence of nanoparticles. The melting point of the polymer did not change with the addition of nanoparticles. The percent crystallinity increased with the presence of nanotubes, showing that this nanofiller acts as a nucleating agent. Table 1 shows that the incorporation of the nanotubes enhanced the thermal stability of the polymers, as the decomposition temperature at 10% weight loss (T_{10}) and the maximum decomposition temperature of the nanocomposites (T_{max}) increased by *ca* 37 °C and 13 °C, respectively, compared to virgin polymers. The incorporation of nanofiller into a polyolefin matrix can act as a superior insulator and mass transport barrier for the volatile products generated during decomposition.[39] Similar results were found when silica nanospheres were incorporated into PP, with T_{max} increasing *ca* 10 °C compared with pure PP. Moreover, a greater increase in thermal stability was found when a compatibilizer was included in the process. The authors concluded that these better results are associated with the presence of the compatibilizer improving the dispersion of the nanoparticles.[3] Changes of the TGA behaviour are strongly influenced by the aspect ratio of the particles and the atmosphere in which the tests are carried out. High

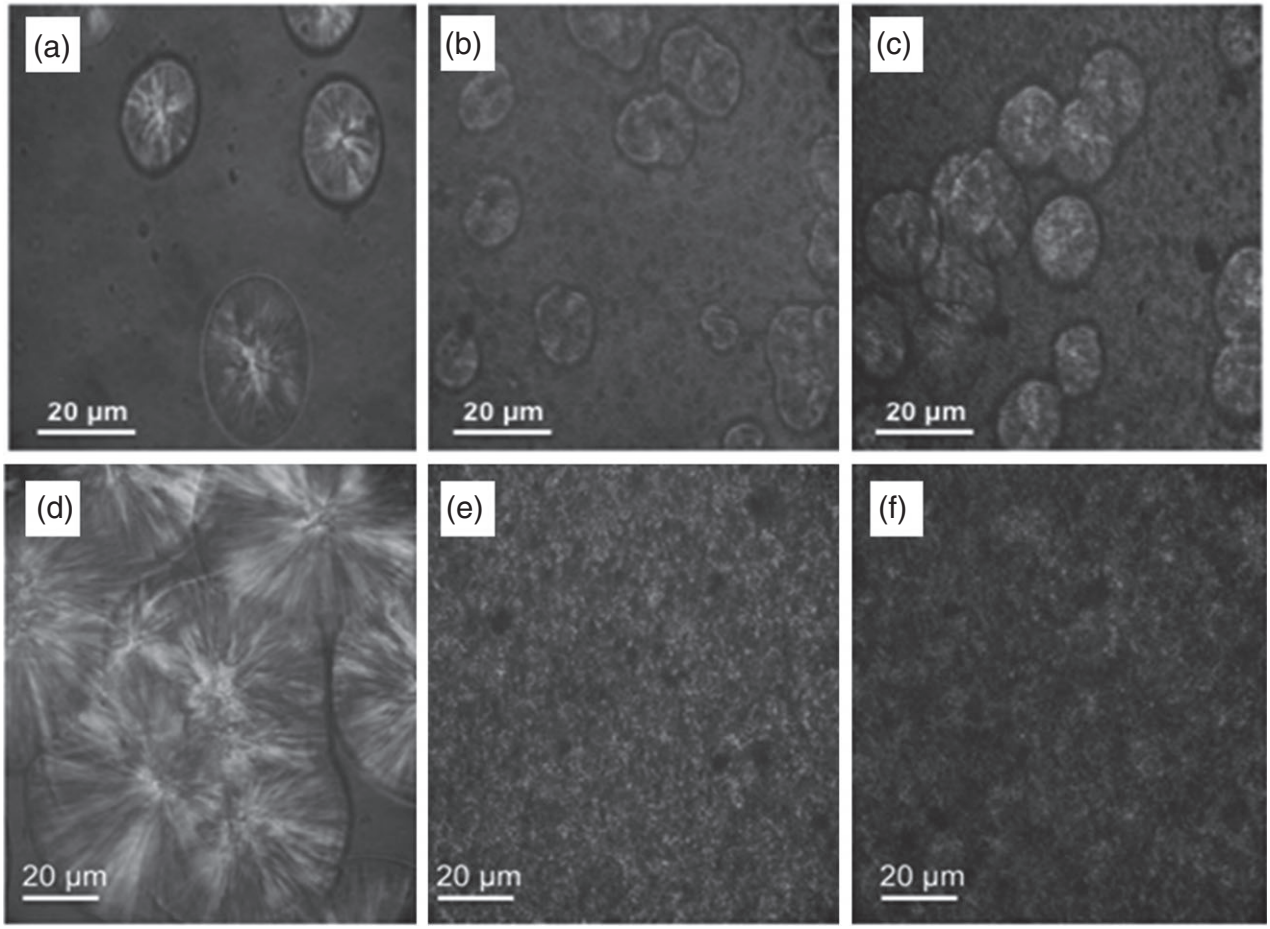

Figure 4. Optical micrographs showing the nucleating effect of TiO_2 nanotubes on PP crystallization at 135 °C: (a) pure PP, (b) PP/TiO_2-Ntbs 5 wt%, (c) PP/Mod-TiO_2-Ntbs 5 wt% at 1.5 min; (d) pure PP, (e) PP/TiO_2-Ntbs 8 wt%, (f) PP/Mod-TiO_2-Ntbs 8 wt% at 4.0 min.

aspect ratio nanoparticles such as clays can increase the thermal stability in an oxygen atmosphere dramatically. Zhang and colleagues[37] studied the thermal stability of PP/montmorillonite composites under a nitrogen atmosphere, showing increases as high as 50 °C in decomposition temperature compared with pure polymer. The authors ascribed the difference to the good dispersion of the layered silicate. On the other hand, Esthappan and Kuttappan[38] showed the variation in the maximum decomposition temperature for PP/TiO_2 nancomposites, where the nanoparticles (nanospheres) were well dispersed in the polymer matrix. The temperature at which maximum degradation took place is increased by 5.36 °C at 3.0 wt% of TiO_2 nanoparticles in comparison with neat PP. They explained the improvement in the thermal stability by the hindered thermal motion of polymer molecular chains. In our case the PP/Mod-TiO_2-Ntb nanocomposites presented slightly higher thermal stability and crystallinity than PP/TiO_2-Ntb nanocomposites. Palza *et al.*[39] further showed that there are several models explaining the improved thermal stability of polymer nanocomposites, which can be due to either chemical or physical processes. From the chemical standpoint, the surface of some nanoparticles can interact with radicals coming from the degradation of the polymer. On the other hand, the physical models are based on the lower diffusivity due to the presence of nanoparticles reducing the out-diffusion of volatile compounds from the decomposition. In our case, both models apply since the TiO_2 surface can interact with radicals coming from the degradation of PP but also, due to their high aspect ratio, nanotubes can reduce the diffusion of volatile compounds.

Spherulite growth rate

The optical images of the spherulites are displayed in Fig. 4 for virgin PP and PP/TiO_2-Ntb nanocomposites with 5 wt% and 8 wt% TiO_2. It is clear that the presence of the particles reduced the diameter of spherulites and in turn increased the number of spherulites, which means a higher nucleation density. This effect is more pronounced with a greater percentage of incorporated nanotubes. At 8 wt% of TiO_2-Ntbs it was impossible to determine the diameter and density of PP spherulites due to their large number and small size.

Figure 5 shows the effect of the incorporation of TiO_2-Ntbs (5 wt%) on the final density of the spherulites. It is clear that the addition of nanotubes increased the number of spherulites per unit area, and that this behaviour was more pronounced when Mod-TiO_2-Ntbs were incorporated.

The presence of the particles in the polymer melt can reduce both the work required to create a new surface and the nucleus size for crystal growth. This behaviour occurs because the interface between the polymer crystal and the filler may be less hindered, so the creation of the corresponding free polymer crystal surface increases the nucleation density of the spherulites.[40] Therefore, a heterogeneous nucleation path reduces the free energy opposing the primary nucleation provided by the pre-existing surface

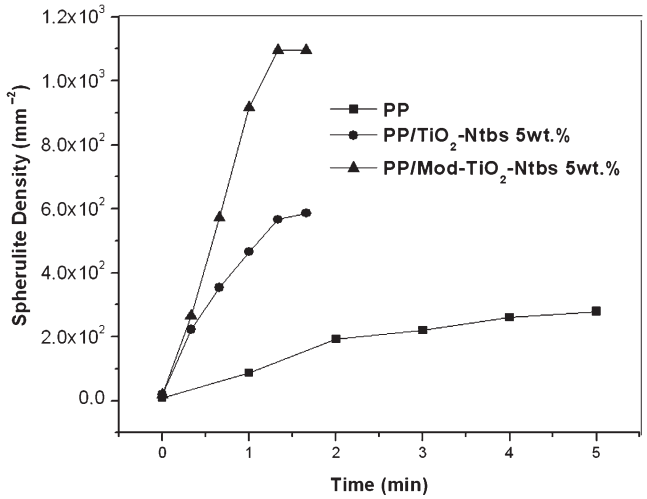

Figure 5. Effect of the incorporation of nanotubes (5 wt%) on the final spherulite density of PP and PP/TiO_2-Ntb nanocomposites.

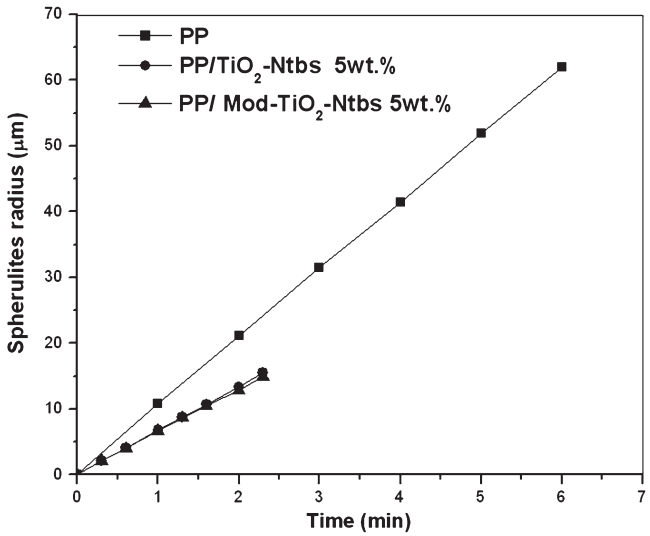

Figure 6. Effect of the incorporation of nanotubes (5 wt%) on the final radius of PP and PP/TiO_2-Ntb nanocomposites.

of the filler. The increased spherulite density can be related to the spatial confinement of the precursor unit between adjacent nanoparticles, hindering the diffusive mobility of precursor unit clusters.[41]

In similar systems, but with silica nanoparticles, the PP spherulite density also increases with the nanofiller, depending largely on particle morphology.[22] In particular, silica nanotubes give rise to the largest changes in morphology compared with other nanoparticles. Our results indicate that the nanotube filler increases the PP spherulite density, which is more pronounced with modified nanotubes.

Figure 6 shows that the spherulite radius of the PP/TiO_2-Ntb nanocomposites is smaller than that of virgin PP. Due to the high density of the spherulites, the time needed to finish this primary crystallization decreases approximately three times with incorporation of the nanotubes. The spherulite radius increased linearly for iPP with time, and it is noteworthy that this linearity is also found for the composites. This linearity shows that titanium nanotubes were accommodated inside the spherulites rather than segregated between the boundaries.[41] The growth rate of the spherulites was determined by the slope of the spherulite radius as a function of time (Fig. 6), with values of 10.3, 6.70 and 6.45 μm min^{-1} for PP, PP/TiO_2-Ntbs and PP/Mod-TiO_2-Ntbs, respectively, showing that the incorporation of titanium inhibits the rate of crystallization compared with virgin PP. The reduction in growth rate has been explained as a decrease in mobility of crystallization units caused by the presence of nanotubes. The growth rate reduction results from spatial confinement of the precursor unit into small volumes between adjacent particles, leading to retardation of the diffusive mobility of the precursors of cluster units.[41]

Table 2. Mechanical properties of PP/TiO_2-Ntb and PP/Mod-TiO_2-Ntb nanocomposites

Process	TiO_2 content (wt%)	E (Mpa)	σ_y (Mpa)	E_{break} (%)
PP	N/A	1181 ± 258	37.2 ± 0.6	9.2 ± 2.1
PP/TiO_2-Ntbs	5%	1257 ± 140	11.6 ± 0.7	6.3 ± 0.6
	8%	1181 ± 93	12.6 ± 1.8	5.4 ± 1.3
PP/Mod-TiO_2-Ntbs	5%	984 ± 123	11.0 ± 1.7	7.9 ± 0.7
	8%	1111 ± 77	13.1 ± 1.8	6.8 ± 0.9

E is Young's modulus; σ_y is the yield stress; E_{break} is the deformation at break.

Mechanical properties

The mechanical properties of PP, PP/TiO_2-Ntbs and PP/Mod-TiO_2-Ntbs composites under tensile tests are displayed in Table 2. Despite both the high aspect ratio and the nano-size of the original filler added, Young's modulus of the composites does not change compared to the pure matrix. However, the yield stress is drastically decreased with the incorporation of nanotubes. There are few previous reports on the mechanical behaviour of similar PP composites, and they show contradictory results about the effect of TiO_2 nanoparticles. Supaphol *et al.* showed that, at low TiO_2 concentrations, PP composites did not change their Young's modulus and only at high concentrations were increases seen.[42] These contradictory results can be explained by the complexity of this kind of two-component system based on a non-polar matrix. The mechanical behaviour of polymer/nanofiller composites is directly related to their hierarchical microstructure that depends on several parameters such as properties of the matrix, properties and distribution of the filler as well as interfacial bonding, and the synthetic or processing methods.[43] For an effective reinforcement, at least four requirements should be addressed: large aspect ratio, good dispersion, alignment and interfacial stress transfer, where dispersion is probably the most fundamental issue.[44] Although it is well known that nanoparticles increase the elastic moduli of a polymer matrix, this is not always observed and the opposite effect can be seen in some systems such as poly(methyl methacrylate)/alumina nanoparticles.[45] In PP/carbon nanotube composites, for instance, there is a filler concentration threshold above which the rise of Young's modulus decreases markedly.[46] The real filler morphology of the agglomerates seems to be the main variable affecting the mechanical behaviour of these composites, and at high concentrations the formation of aggregates decreases the interfacial filler/polymer adhesion, thereby decreasing the effect. In this case, the aggregates of nanotube ropes effectively reduce the aspect ratio of the reinforcement. The slipping of the

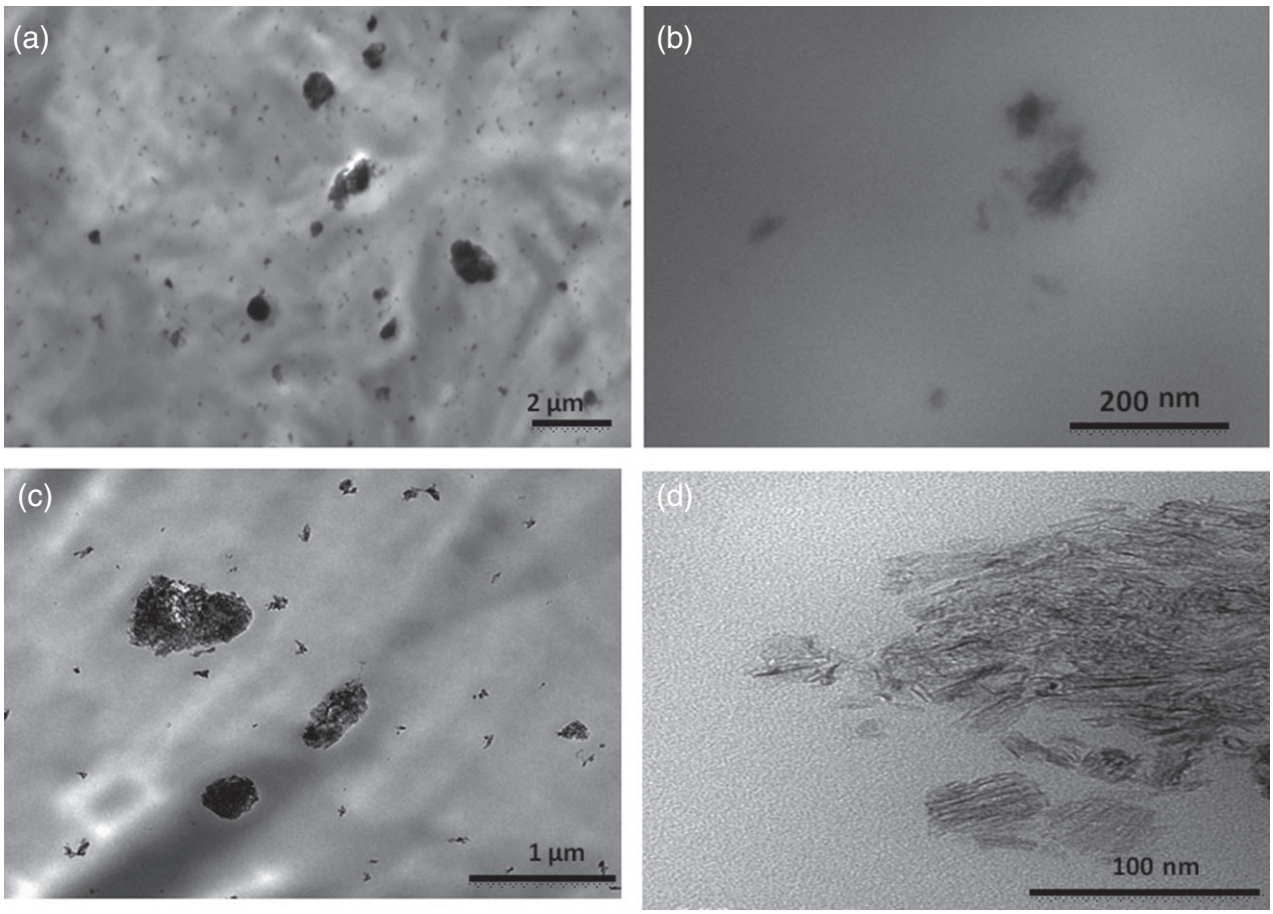

Figure 7. TEM images of (a), (b) PP/TiO_2-Ntbs; (c), (d) PP/Mod-TiO_2-Ntb nanocomposites with a 5 wt% load.

nanotubes when they are assembled in ropes further affects the elastic properties of the composite.[47] PP filled with nanometric rod-like cellulose whiskers can either decrease or increase Young's modulus depending on the degree of dispersion of the particles.[48] At high aggregation, zones with accentuated fragility are created leading to brittleness in this material. These tensile results and the lack of compatibility between the whiskers and the matrix led to the conclusion that there was very little or no stress transfer of properties. Some PP/clay nanocomposites can also show unexpected mechanical behaviours such as lower tensile yield stress than the pure matrix due to poor interfacial interactions.[49] This low interaction between the polymer and the filler has also justified a slight decrease in the elastic modulus of some PE composites filled with metal nanoparticles.[50] Therefore, both the polymer – particle interaction and the agglomeration state of the filler drive the final effect of the nanoparticle on the mechanical behaviour of the composite.

As above mentioned, Altan *et al.*[19] observed a decrease in the yield stress of *ca* 70% for PP/TiO_2 nanocomposites. These results were due to the poor interfacial adhesion between the TiO_2 nanoparticles and the matrix. Nguyen *et al.*[10] otherwise reported that the mechanical properties of PE increased with a TiO_2 nanoparticle load in the range 0.5 – 2 wt%. However, when the load of TiO_2 nanoparticles was higher than 3 wt%, the mechanical properties decreased with respect to neat PP. This behaviour was attributed to the agglomeration of TiO_2 nanoparticles at relatively high filler contents. Our group recently reported that when 5 wt% of TiO_2 nanospheres was incorporated into high density PE Young's modulus did not change, but when incorporated into a 'quasi-elastomeric' PE this property increased.[7]

To understand our mechanical results, the morphology of the composites was analysed by electron microscopy. In particular, TEM images of the PP/TiO_2-Ntb and PP/Mod-TiO_2-Ntb nanocomposites containing 5 wt% filler load were analysed. The results are shown in Fig. 7. In general, individual high aspect ratio nanoparticles are not seen in the PP matrix and mainly well distributed secondary structures with sizes around 100 nm are displayed. Moreover, there are some regions showing large agglomerates with sizes around 1 µm. Comparing the TEM images in Fig. 1 with those in Fig. 7 it is concluded that there is rupture of the original bundles of TiO_2-Ntbs. Therefore, these results show that the real aspect ratio of the nanoparticle as a consequence of the melt mixing process is drastically reduced and globular particles or aggregates are mainly seen in the composites rather than tube-like individual fillers. The surface modification of the particles does not have a relevant effect on the filler distribution in the polymer matrix, being consistent with the similar mechanical values reported in Table 2.

Based on the above results, we can state that our composites do not show any improvement in Young's modulus due to both poor interfacial interaction between the filler and the non-polar matrix and a low aspect ratio of the final particles or agglomerates. The high degree of agglomeration of the filler should also be considered at this point. This lack of polymer – filler interaction can also explain the drastic decrease in the yield stresses of our composites.

Table 3. Biocidal properties against *E. coli* of nanocomposites irradiated with white light and UVA light

Sample	TiO_2 content (wt%)	Irradiation	Reduction (%)
PP	–	White light	–
	–	UVA	–
PP/TiO_2-Ntbs	5%	White light	17
	5%	UVA	75
PP/Mod-TiO_2-Ntbs	5%	White light	25
	5%	UVA	81

Morphological characterization of nanocomposites

TEM images of the PP/TiO_2-Ntb and PP/Mod-TiO_2-Ntb nanocomposites containing 8 wt% filler load are shown in Fig. 7. In general, well distributed TiO_2 nanoparticles form secondary structures with sizes around 100 nm in the PP matrix. However, there were some regions showing large agglomerates with sizes around 1 μm. These images further show the negligible effect of the nanoparticle organic modification on filler dispersion.

Biocidal properties

The results of the antimicrobial tests against *E. coli* in CFU and their percentage reduction with respect to virgin PP, irradiated with white light and UVA radiation for 4 h, are shown in Table 3. PP/TiO_2-Ntbs and PP/Mod-TiO_2-Ntbs composites with 5 wt% of filler showed a slight CFU reduction of 17% and 25%, respectively, against *E. coli* compared to neat PP when they were irradiated with white light. This behaviour improved when the composites were irradiated with UVA radiation, resulting in 75% and 81% reduction of CFU for PP/TiO_2-Ntb and PP/Mod-TiO_2-Ntb composites, respectively. The greater *E. coli* CFU reduction after UVA irradiation of the composites is due to the reactive species generated by the photocatalysis processes occurring in the TiO_2 particles in the presence of water, such as OH, O_2^- and H_2O_2. Such species are capable of interacting with and degrading the outer membrane of the bacteria and then easily reaching the cytoplasmic membrane, which leads to peroxidation of membrane lipids followed by death of the cells.[51,52]

Although TiO_2-Ntbs have a slightly higher energy band gap than nanospheres, and therefore a more stable photocatalytic activity, the biocidal properties of PP/TiO_2-Ntbs reached 75%. On the other hand, in previous work we found that when TiO_2 nanospheres were incorporated into the PE matrix bacterial reduction rose to 99.99%.[14] This result can be due to the nanoparticle morphology and matrix effects that have an influence on the biocidal properties. For example, nanospheres can travel more easily through the amorphous part of the polymer to reach the surface and form active species, but nanotubes are prevented from going through these processes due to their high aspect ratio. It was reported that either the crystallinity or the morphology of the polymer has an influence on the biocidal activity. Our group studied the biocidal properties of two different PEs, high density polyethylene (HDPE) and linear low density PE (LLDPE), filled with TiO_2 nanotubes (O-TiO_2-Ntb). For PE/O-TiO_2-Ntb and LLDPE/O-TiO_2-Ntb nanocomposites, the reduction against *E. coli* after 2 h of exposure was 43.1% and 99.9%, respectively. This behaviour can be ascribed to the higher crystallinity of PE compared with LLDPE, as the irradiated light can penetrate more easily in the amorphous zones of LLDPE. On the other hand, the nanoparticles can also travel more easily in the amorphous part of LLDPE than in PE, favouring nanoparticle diffusion to the surface of the film. Afterwards, in contact with oxygen and humidity, the active species are generated and therefore high biocidal properties against *E. coli* are observed.[53]

CONCLUSIONS

A hydrothermal method was used to produce TiO_2-Ntbs, which were then modified organically with hexadecyltrimethoxysilane (Mod-TiO_2-Ntbs). The nanoparticle modification did not improve the mechanical properties, although the use of the modified nanotubes as filler in PP improved the thermal stability and the crystallization process of the polymer. The incorporation of nanotubes gives biocidal properties to the PP, regardless of which filler is embedded in the matrix. Furthermore, the biocidal properties depend on the type of irradiation. The PP/TiO_2 nanocomposites irradiated with UVA had a biocidal activity of 75% against *E. coli*, which increased to 81% with organic modification of the TiO_2-Ntbs filler. Therefore, although the modification of the nanoparticles did not improve the mechanical properties, it resulted in a PP with a better biocidal character.

ACKNOWLEDGEMENTS

P. A. Zapata acknowledges the financial support by FONDECYT under Iniciación en Investigación Project 11110237 and by the Departamento de Investigaciones Científicas y Tecnológicas, DICYT, of the Universidad de Santiago de Chile.

REFERENCES

1 Paul DR and Robeson LM, *Polymer* **49**:3187–3204 (2008).
2 Palza H, Reznik B, Kappes M, Hennrich F, Naue IFC and Wilhelm M, *Polymer* **51**:3753–3761(2010).
3 Palza H, Vergara R and Zapata PA, *Comp Sci Technol* **71**:535–540 (2011).
4 Zapata PA, Quijada R, Covarrubia C, Moncada E and Retuert J, *J Appl Polym Sci* **113**:2368–2377 (2009).
5 Zapata OA and Quijada R, *J Nanomater* 2012: art. 194543 (2012).
6 Fim FdC, Gutierres JM, Basso NRS and Galland GB, *J Polym Sci A Polym Chem* **48**:692–698 (2010).
7 Zapata PA, Palza H, Cruz LS, Lieberwirth I, Catalina F, Corrales T *et al.*, *Polymer* **54**:2690–2698 (2013).
8 Pozo I, Olmos D, Orgaz B, Božanić DK and González-Benito J, *Mater Lett* **127**:1–3 (2014).
9 Dastjerdo R and Montazerr M, *Colloids Surf B Biointerfaces* **79**:5–18 (2010).
10 Nguyen V, Thai H, Mai D, Tran H, Tran D and Vu M, *Compos B Eng* **45**:1192–1198 (2013).
11 Zhang M, Bando Y and Wada K, *J Mater Sci Lett* **20**:167–170 (2001).
12 Zapata PA, Palza H and Rabagliati FM, *J Polym Sci A Polym Chem* **50**:4055–4062 (2012).
13 Džunuzović E, Vodnik E, Jeremić K and Nedeljkovićv JM, *Mater Lett* **63**:908–910 (2009).
14 Velásquez J, Valencia S, Rios L, Restrepo G and Marín J, *Chem Eng J* **203**:398–405 (2012).
15 Esthappan S, Kuttapan S and Joseph R, *Mater Design* **37**:537–542 (2012).
16 Kubacka A, Ferrer M, Cerrada M, Serrano C, Sánchez-Chaves M, Fernández-García M *et al.*, *Appl Catal B* **89**:441–447 (2009).
17 Chawengkijwanich C and Hayata Y, *Int J Food Microbiol* **123**:288–292 (2008).
18 Maneerat C and Hayata Y, *Int J Food Microbiol* **107**:99–103 (2006).
19 Altan M and Yildirim H, *J Mater Sci Technol* **28**:686–692 (2012).
20 Zohrevand A, Ajji A and Mighri F, *Polym Eng Sci* **54**:874–886 (2014).
21 Mikešová J, Šlouf M, Gohs M, Popelková D, Vacková T, Hung Vu N *et al.*, *Polym Bull* **71**:795–818 (2014).

22 Palza H, Vera J, Wilhelm M and Zapata PA, *Macromol Mater Eng* **29**:6744–6751 (2011).
23 Kasuga T, Hiratmasu M, Hoson A, Sekino T and Niihara K, *Langmuir* **14**:3160–3163 (1998).
24 Salinas D, Araya P and Guerrero S, *Appl Catal B* **117**:260–267 (2012).
25 Abdelmouleh M, Boufi S, Naceur Belgacem M, Dufresne A and Gandini A, *J Appl Polym Sci* **98**:974–984 (2005).
26 Wang W, Fan Z, Zhu Y, Zhang Y and Feng L, *Eur Polym J* **38**:1551–1558 (2002).
27 Zapata PA, Quijada R and Benavente R, *J Appl Polym Sci* **119**:1771–1780 (2011).
28 Ansari S, Pazouki M and Hosseinnia A, *Powder Technol* **196**:241–245 (2009).
29 Khanna PK, Singh N and Charan S, *Mater Lett* **61**:4725–4730 (2007).
30 Nian JN, Chen SA, Tsai CC and Teng H, *J Phys Chem B* **110**:25817–25824 (2006).
31 Guerrero S, Diserio M, Li RF and Wolf E, *Catal Lett* **130**:19–27 (2009).
32 László K and Imre D, *Colloids Surf A Physicochem Eng Asp* **280**:146–154 (2006)
33 Mejia MI, Marín JM, Restrepo G, Rios LA and Pulgarín C, *Appl Catal B* **94**:166–172 (2010).
34 Abdelmouleha M, Boufia S, Belgacemb MN, Duartec AP, Ben Salaha A and Gandini A, *Int J Adh Adhes* **24**:43–54 (2004).
35 Xie Y, Hill CAS, Xiao Z, Militz H and Mai C, Compos A *Appli Sci Manuf* **41**:806–819 (2010).
36 Abdelmouleha M, Boufia S, Belgacemb MN, Duartec AP, Ben-Salaha A and Gandinib A, *Int J Adh Adhes* **24**:43–54 (2004).
37 Quin H, Zhang S, Zhao C, Feng M, Yang M, Shu Z *et al.*, *Polym Degrad Stab* **85**:807–813 (2004).
38 Esthappan SK and Kuttappan JR, *Polym Degrad Stab* **97**:615–620 (2012).
39 Palza H, Vergara R and Zapata PA, *Macromol Mater Eng* **295**:899–905 (2010).
40 Mucha M and Królikowski Z, *J Therm Anal Calorim* **74**:549–557 (2003).
41 Nitta K, Asuka K, Liu B and Terano M, *Polymer* **47**:6457–6463 (2006).
42 Supaphol P, Thanomkiat P, Junkasem J and Dangtungee R, *Polym Test* **26**:20–37 (2007).
43 Tjong SC, *Mater Sci Eng R Rep* **53**:73–197 (2006).
44 Coleman JN, Khan U, Blau WJ and Gun'ko YK, *Carbon* **44**:1624–1652 (2006).
45 Ash BJ, Rogers DF, Wiegand CJ, Schadler LS, Siegel RW, Benicewicz BC *et al.*, *Polym Compos* **23**:1014–1025 (2002).
46 Lopez Manchado MA, Valentini L, Biagiotti J and Kenny JM, *Carbon* **43**:1499–1505 (2005).
47 Salvetat P, Briggs GAD, Bonard JM, Bacsa RR, Kulik AJ and Stockli T, *Phys Rev Lett* **82**:944–947 (1999).
48 Ljungberg N, Cavaille JY and Heux L, *Polymer* **47**:6285–6292 (2006).
49 Pozsgay A, Frater T, Szazdi L, Muller P, Sajo I and Pukanszky B, *Eur Polym J* **40**:27–36 (2004).
50 Luyt AS, Molefi JA and Krump H, *Polym Degrad Stab* **91**:1629–1636 (2006).
51 Sunada K, Watanabe T and Hashimoto K, *J Photochem Photobiol A Chem* **156**:227–233 (2003).
52 Huang Z, Maness PC, Blake DM, Wolfrum EJ, Smolinski SL and Jacoby WA, *J Photochem Photobiol A Chem* **130**:163–170 (2000).
53 Yañez D, Rabagliati FM, Guerrero S, Lieberwirth I, Ulloa MT, Gomez T *et al.*, *Appl Catal A* **489**:255–261 (2015).

